

International Journal of Research in Pharmacy and Science

3D QSAR Analysis on Triazepane Derivatives as DPP-IV Inhibitors

Patil Swaraj^{1*}, Prajapati Amit¹, Ansari Khusbu², Khodre Suraj³,
Choudhary Shrikant²

¹Department of Pharmaceutical Chemistry, KLE universitys College of Pharmacy
Rajajinagar, Bangalore, India

²LNCT, Raisen Road, Bhopal, Madhya Pradesh, India,

³Ayurveda College, Rewa, Madhya Pradesh, India

ABSTRACT

Three dimensional quantitative structure activity relationship (3D QSAR) analysis using k nearest neighbor molecular field analysis (kNN MFA) method was performed on a series of Triazepane derivatives as dipeptidyl peptidase IV (DPP IV) inhibitors using molecular design suite (VLifeMDS). This study was performed with 22 compounds (data set) using sphere exclusion (SE) algorithm method for the division of the data set into training and test set. KNN-MFA methodology with stepwise (SW), simulated annealing (SA) and genetic algorithm (GA) was used for building the QSAR models. The predictive models were generated with SW-kNN MFA. The most significant model is having internal predictivity 72.62% ($q^2 = 0.7262$) and external predictivity 47.06 % ($pred_r^2 = 0.4706$).

KEYWORDS: 3D-QSAR, kNN-MFA, simulated annealing, DPP IV inhibitors, genetic algorithm ,
Triazepane derivatives

***Corresponding Author**

Swaraj Patil

Project Assistant DAVV School of Pharmacy,

Indore, Madhya Pradesh, India

Mobile No. 917415361595

E-mail: swarajpatil2006@gmail.com

INTROUCTION

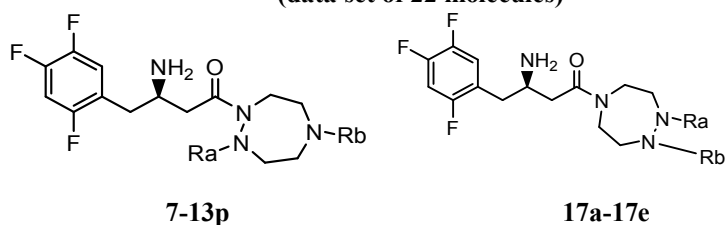
DPP-4 preferentially cleaves incretin hormones, GLP-1 and GIP peptides with the amino acid alanine or proline in position 2 of the N-terminus of the peptide chain. Active GLP-1(7–36) amide was cleaved by DPP-4 to yield a dipeptide (His-Ala) and GLP-1(9–36)amide.¹⁻³ DPP-4 is also present on the cell membrane of activated T lymphocytes as CD26⁴; however, there is no evidence found which shows that the catalytic activity of the enzyme is important in immune function. In clinical studies with DPP-4 inhibitors, no serious side effects or adverse events on immunological regulatory mechanisms have been observed.⁵ Recently, 2-year safety data on sitagliptin from pooled clinical trials have been published.⁶ Alogliptin and saxagliptin are currently under review for approval, and other DPP-4 inhibitors are in development.⁷⁻¹⁰ Prevention of inactivation of glucagon-like peptide-1 (GLP-1) by inhibition of the enzyme dipeptidyl peptidase-4 (DPP-4) is a strategy that is currently being developed as a novel treatment for type 2 diabetes.¹¹⁻¹³ DPP-4 inhibition has thereby been demonstrated to be anti-diabetic both in animal models of diabetes¹⁴⁻¹⁵ and in patients with type 2 diabetes.¹⁶⁻¹⁷

MATERIAL AND METHOD

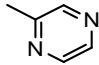
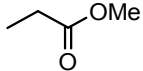
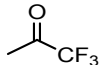
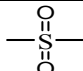
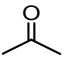
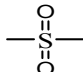
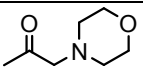
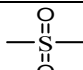
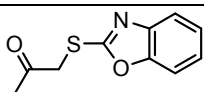
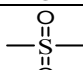
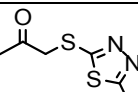
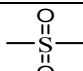
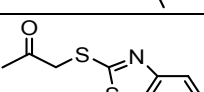
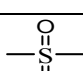
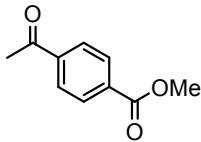
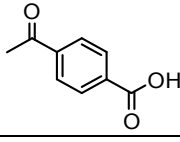
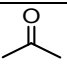
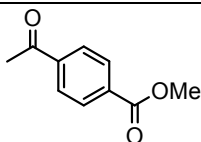
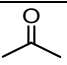
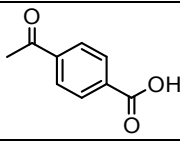
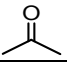
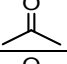
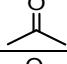
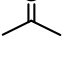
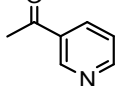
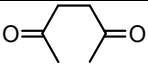
Data Set:

Study data set of Triazepane derivatives (22 molecules)¹⁸ has been taken from the literature for QSAR studies reported in table 1. The reported IC₅₀ values (nM), have been changed to the logarithmic scale [pIC₅₀ (moles)], for QSAR study.

Table 1: General structure of the compounds of cyanopyrrolidine derivatives and their biological activities (data set of 22 molecules)



S. No.	Compound	Ra	Rb	IC ₅₀ (nM)	log(1/IC ₅₀)
1	7	H	H	9800	5
2	13a	H		859	6.06
3	13b			578	6.23
4	13c			1200	5.92

5	13d	H		2500	5.6
6	13e	H		2900	5.53
7	13f	H		681	6.16
8	13g	H		609	6.21
9	13h			1800	5.74
10	13i			700	6.15
11	13j			401	6.39
12	13k			591	6.22
13	13l			151	6.82
14	13m	H		439	6.35
15	13n	H		216	6.66
16	13o			213	6.67
17	13p			98	7
18	17a	H	H	4500	5.34
19	17b		H	3300	5.48
20	17c			1600	5.79
21	17d			660	6.18
22	17e			853	6.06

Molecular Modeling Study:

Molecular modeling and kNN-MFA study was performed on HP computer having genuine Intel Pentium Dual Core Processor and Windows XP operating system using the software Molecular Design Suite (MDS).¹⁹ The selected dataset were aligned by using template based alignment method. The alignment of all the molecules on the template is shown in figure 1.

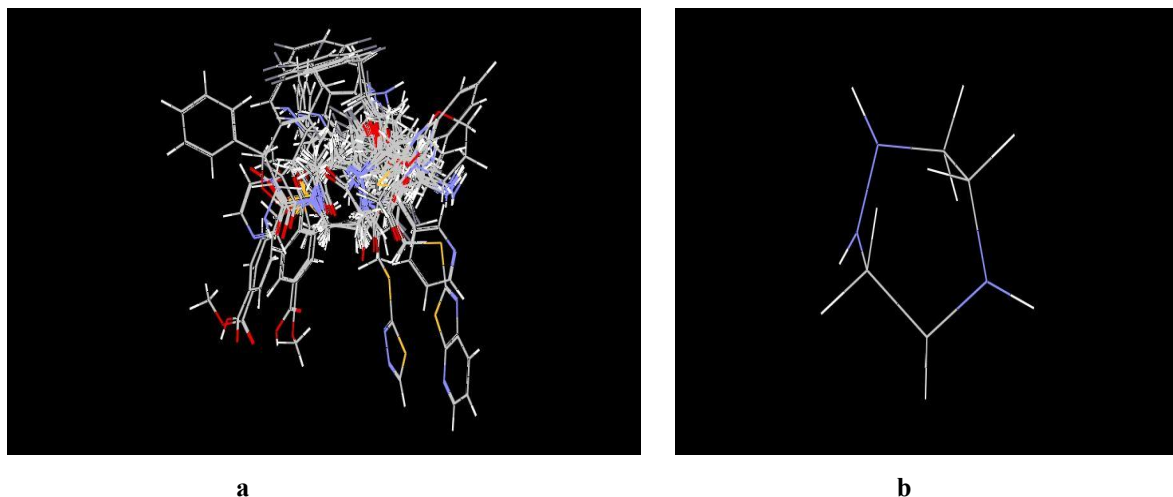


Figure 1: The alignment of all the molecules (a) on the template (b)

Descriptor calculation:

Once the molecules are aligned, a molecular field is computed on a grid of points in space around the molecule. This field provides a description of how each molecule will tend to bind in the active site. Descriptors representing the steric and electrostatic interaction energies were computed at the lattice points of the grid using a methyl probe of charge +1.

Data selection:

In order to evaluate the QSAR model externally, data set was divided into training and test set using sphere exclusion methods. Training set is used to develop the QSAR model for which biological activity data are known. Test set is used to challenge the QSAR model developed based on the training set to assess the predictive effectiveness of the model which is not included in model generation. Sphere exclusion algorithm was used for creation of training and test sets. Sphere exclusion algorithm²⁰ allows constructing training sets covering all descriptor space areas occupied by representative points. The higher the dissimilarity level, the smaller the training set is and the larger the test set is and vice versa. It is expected that the predictive ability of QSAR models generally decrease when the dissimilarity level increases. Once the training and test sets are generated, kNN methodology

is applied to descriptors generated over grid. Random selection method was also used to construct and validate the QSAR models, both internally and externally.

Model Building:

Models were generated by k nearest neighbor molecular field analysis (kNN-MFA) in conjunction with stepwise (SW) forward-backward, simulated annealing (SA) and genetic algorithm (GA) variable selection methods with pIC50 activity field as dependent variable and descriptors as independent variable²¹⁻²³ is shown in table 2.

Table 2: Result of kNN-MFA study using sphere exclusion selection method

S. No	Dissimilarity value	Test set	SW-kNN MFA		GA-kNN MFA		SA-kNN MFA	
			q2	Predr2	q2	Predr2	q2	Predr2
1	8	07, 13e	0.6462**	0.0692	0.1866	-0.3288	0.5778*	0.1025
2	9.5	07, 13e, 17a, 17d	0.5567*	-0.8225	0.0649	0.2269	0.7262**	0.3889
3	10	07, 13e, 13g, 17a, 17d	0.5610*	-0.8376	0.1871	0.2697	0.6801*	0.0790
4	11	07, 13d, 13e, 13g, 17a, 17c	0.6134**	0.1608	0.1613	0.0566	0.54218	0.3882
5	12	07, 13d, 13e, 13g, 13h, 17a, 17c	0.4268*	-0.2885	0.1738	-0.2529	0.4535*	0.4706
6	13	07, 13d, 13e, 13g, 13h, 13o, 17a, 17c	0.6225**	-0.0264	-0.0214	0.3174	0.5404*	0.1845
7	14	07, 13c, 13d, 13e, 13g, 13h, 13m, 13o, 17a, 17c, 17d	0.4075*	0.3369	0.1396	-0.0793	0.5298*	0.1372

RESULTS AND DISCUSSION

Different training and test set of Triazepane derivatives were constructed using sphere exclusion (dissimilarity level 8 to 14) table 2. Training and test set were selected if they follow the Unicolumn statistics table 3, i.e., maximum of the test is less than maximum of training set and minimum of the test set is greater than of training set, which is prerequisite for further QSAR analysis shown in table 3. This result shows that the test is interpolative i.e., derived from the min-max range of training set.

Table 3: Uni-Column Statistics for training and test set activity

Column Name	Average	Max	Min	Std Dev	Sum
Training set	6.1515	7.0000	5.3400	0.4347	123.0300
Test set	5.2650	5.5300	5.5000	0.3748	10.5300

The mean and standard deviation of the training and test set provides insight to the relative difference of mean and point density distribution of the two sets. k-Nearest neighbor molecular field analysis (kNN-MFA) was applied using stepwise (SW), simulated annealing (SA) and genetic algorithm (GA) approaches for building QSAR models. Results of models developed by SW-kNN MFA, SA-kNN MFA and GA-kNN MFA using sphere exclusion methods shown in table 2. Actual and predicted biological activity for Training set and test set shown in table 4.

Table 4: Actual and predicted biological activity for Training set and test set

S. No	Compound	Actual	Predicted		
			SW-KNN MFA	GA-KNN MFA	SA-KNN MFA
1	7	5	6.07879	6.34846	6.19859
2	13a	6.06	6.08685	5.72722	6.10035
3	13b	6.23	6.30462	5.98357	5.99974
4	13c	5.92	6.25996	5.94893	6.14712
5	13d	5.6	5.67846	6.2742	6.17654
6	13e	5.53	6.18572	6.20594	5.84641
7	13f	6.16	5.83671	5.95157	5.98355
8	13g	6.21	5.96937	5.92507	5.88406
9	13h	5.74	5.69213	6.07997	5.44758
10	13i	6.15	6.1702	5.97746	6.11917
11	13j	6.39	6.13252	6.26975	6.675
12	13k	6.22	6.51683	6.7129	6.07569
13	13l	6.82	6.36413	6.22931	6.85883
14	13m	6.35	6.41438	6.47012	6.66
15	13n	6.66	6.33204	6.42097	6.35
16	13o	6.67	6.34148	6.59236	6.5475
17	13p	7	6.66987	6.32681	6.57559
18	17a	5.34	5.65119	5.98502	5.54966
19	17b	5.48	5.61762	5.84155	5.38749
20	17c	5.79	5.89489	6.02084	6.17999
21	17d	6.18	5.97613	5.82275	5.79
22	17e	6.06	6.40309	5.66238	6.13342

Data fitness plot of stepwise (SW), simulated annealing (SA) and genetic algorithm (GA) is shown in figure 2a, 2b and 2c.

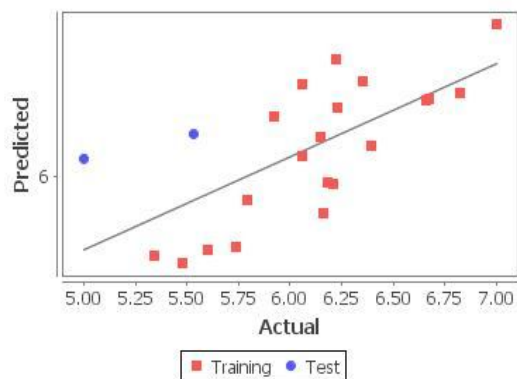


Figure 2a: Fitness plot stepwise (SW)

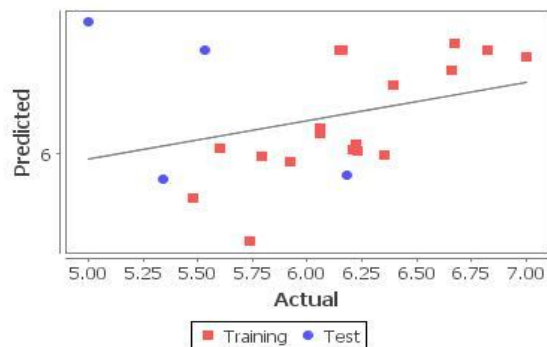


Figure 2b: Fitness plot simulated annealing (SA)

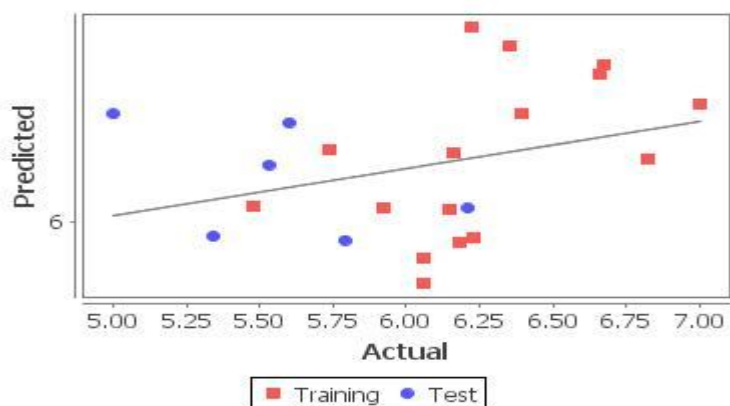


Figure 2c: Fitness plot genetic algorithm (GA)

Result of the observed and predicted biological activity for the training and test compounds for the Model is shown in table 4. The plot of observed vs. predicted activity of training and test sets for stepwise (SW), simulated annealing (SA) and genetic algorithm (GA) is shown in figure 3, 4 and 5.

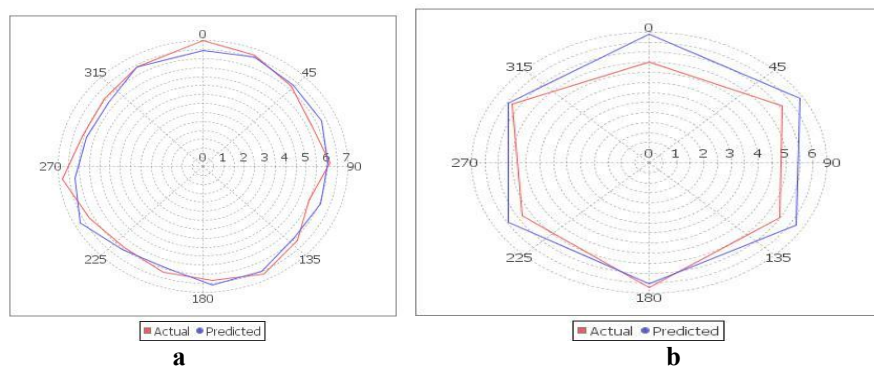


Figure 3: predicted activity of training (a) and test (b) sets for genetic algorithm (GA)

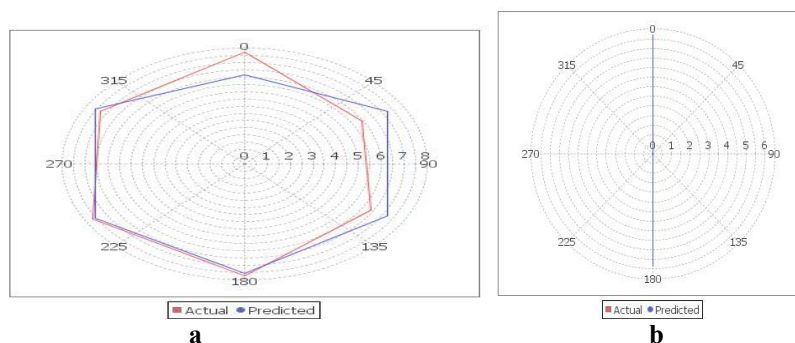


Figure 4: predicted activity of training (a) and test (B) sets for simulated annealing (SA)

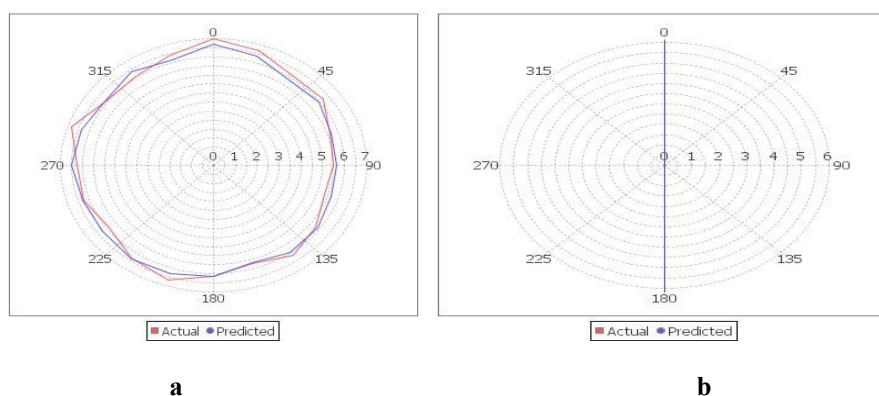


Figure 5: predicted activity of training (a) and test (b) sets for stepwise (SW)

From the plot it can be seen that kNN-MFA model is able to predict the activity of training set quite well (all points are close to regression line) as well as external. Sphere exclusion (SE) algorithm and random selection methods were used for constructing training and test sets. kNN-MFA methodology with stepwise (SW), simulated annealing (SA) and genetic algorithm (GA) was used for building the QSAR models.

In the present data set, SA-kNNMFA and SW-kNN-MFA method does not result in any predictive model. The predictive models were generated with SW-kNN MFA. The most significant model is having internal predictivity 72.62% ($q^2 = 0.7262$) and external predictivity 47.06 % ($\text{pred}_r2 = 0.4706$).

REFERENCE

1. Mentlein R. Dipeptidyl-peptidase IV (CD26)–role in the inactivation of regulatory peptides. *Regulatory Peptides*. 1999; 85: 9–24.
2. Gault VA, Parker JC, Harriott P et al. Evidence that the major degradation product of glucose-dependent insulinotropic polypeptide, GIP(3–42), is a GIP receptor antagonist in vivo. *The Journal of Endocrinology*. 2002; 175: 525–533.

3. Knudsen LB & Pridal L. Glucagon-like peptide-1-(9–36) amide is a major metabolite of glucagon-like peptide-1-(7–36) amide after in vivo administration to dogs, and it acts as an antagonist on the pancreatic receptor. *European Journal of Pharmacology*. 1996; 318: 429–435.
4. De Meester I, Korom S, Van Damme J et al. CD26, let it cut or cut it down. *Immunology Today*. 1999; 20: 367–375.
5. Drucker DJ & Nauck MA. The incretin system: glucagon-like peptide-1 receptor agonists and dipeptidyl peptidase-4 inhibitors in type 2 diabetes. *Lancet*. 2006; 368: 1696–1705.
6. Williams-Herman D, Round E, Swern AS et al. Safety and tolerability of sitagliptin in patients with type 2 diabetes: a pooled analysis. *BMC Endocrine Disorders*. 2008; 8: 14.
7. Gallwitz B. Saxagliptin, a dipeptidyl peptidase IV inhibitor for the treatment of type 2 diabetes. *IDrugs*. 2008; 11: 906–917.
8. Deacon CF. Alogliptin, a potent and selective dipeptidyl peptidase-IV inhibitor for the treatment of type 2 diabetes. *Current Opinion in Investigational Drugs*. 2008; 9: 402–413.
9. Huttner S, Graefe-Mody EU, Withopf B et al. Safety, tolerability, pharmacokinetics, and pharmacodynamics of single oral doses of BI 1356, an inhibitor of dipeptidyl peptidase 4, in healthy male volunteers. *Journal of Clinical Pharmacology*. 2008; 48: 1171–1178.
10. Deacon CF, Ahrén B, Holst JJ. Inhibitors of dipeptidyl peptidase IV: a novel approach to prevention and treatment of type 2 diabetes. *Expert Opin Investig Drugs*. 2004; 13: 1091–102.
11. Ahrén B. Inhibition of dipeptidyl peptidase-4 (DPP-4)—a novel approach to treat type 2 diabetes. *Curr Enzyme Inhib*. 2005; 1: 65–73.
12. Barnett A. DPP-4 inhibitors and their potential role in the management of type 2 diabetes. *Int J Clin Pract*. 2006; 60: 1454–70.
13. Ahrén B, Holst JJ, Mårtensson H, Balkan B. Improved glucose tolerance and insulin secretion by inhibition of dipeptidyl peptidase IV in mice. *Eur J Pharmacol*. 2000; 404: 39–45.
14. Balkan B, Kwasnik L, Miserendino R, Holst JJ, Li X. Inhibition of dipeptidyl peptidase IV with NVP DPP728 increases plasma GLP-1 (7-36 amide) concentrations and improves oral glucose tolerance in obese Zucker rats. *Diabetologia*. 1999; 42: 1324–31.
15. Kvist Reimer M, Holst JJ, Ahrén B. Long-term inhibition of dipeptidyl peptidase IV improves glucose tolerance and preserves islet function in mice. *Eur J Endocrinol*. 2002; 146: 717–27.
16. Pedersen RA, White HA, Schlenzig D, Pauly RP, McIntosh CHS, Dermuth HU. Improved glucose tolerance in Zucker fatty rats by oral administration of the dipeptidyl peptidase IV inhibitor isoleucine thiazolidide. *Diabetes*. 1998; 47: 1253–8.

17. Ahrén B, Gomis R, Standl E, Mills D, Schweizer A. Twelve-and 52-week efficacy of the dipeptidyl peptidase IV inhibitor LAF237 in metformintreated patients with type 2 diabetes. *Diabetes Care*. 2004; 27: 2874–80.
18. Woul SP, Mi AJ, Mi SS, Sung WK, etal. Synthesis and biological evaluation of triazepane derivatives as DPP-IV inhibitors. *Journal of Fluorine Chemistry*. 2009; 130: 1001–1010.
19. VLifeMDS 3.0, Molecular Design Suite, Vlife Sciences Technologies Pvt. Ltd., Pune, India (2004), www.vlifesciences.com.
20. Shen M, LeTiran A, Xiao Y, Golbraikh A, Kohn H and Tropsha A, Quantitative Structure–Activity Relationship Analysis of Functionalized Amino Acid Anticonvulsant Agents Using k Nearest Neighbor and Simulated Annealing PLS Methods, *J. Med. Chem*. 2002; 45: 2811-2823.
21. Zheng W, Topsha A. Novel variable selection quantitative structure—property relationship approach based on the k-nearestneighbor principle, *J Chem Inf Comput Sci*. 2000; 40: 185-194.
22. Ajmani S, Kamaiakar J and Kulkarni SA, Three-Dimensional QSAR Using the k- Nearest Neighbor Method and Its Interpretation, *J Chem. Inf. Model* 2006; 46: 24-31.
23. Rogers D, Hopfinger AJ. Application of Genetic Function Approximation to Quantitative Structure-Activity Relationships and Quantitative Structure-Property Relationships, *J. Chem. Inf. Comp. Sci*. 1994; 34: 854-866